

PHYSICAL REVIEW D

PARTICLES AND FIELDS

THIRD SERIES, VOL. 4, NO. 11

1 December 1971

Absorption Cross Sections of K^+ and \bar{p} on Carbon and Copper in the Region 1.0–3.3 GeV/c*

R. J. Abrams,† R. L. Cool,‡ G. Giacomelli,§ T. F. Kycia, B. A. Leontic,||

K. K. Li, A. Lundby,** D. N. Michael, and J. Teiger††

Brookhaven National Laboratory, Upton, New York 11973

(Received 27 August 1971)

Measurements of K^+ -meson and \bar{p} absorption cross sections on carbon and copper in the region 1.0–3.3 GeV/c are presented.

In this note we shall discuss the measurements of absorption cross sections of K^+ mesons and \bar{p} 's on carbon and copper in the region 1.0–3.3 GeV/c. The measurements were made in the course of two experiments to measure the total cross sections of K^+ mesons and \bar{p} 's in hydrogen and deuterium.^{1,2} Cross sections in complex nuclei are useful in high-energy experiments, for instance, for computing regeneration effects in the neutral K -meson amplitudes,³ or for correcting data for absorption in target vessels and other apparatus.⁴ In recent years there has been an increase in interest in high-energy cross sections in complex nuclei for nuclear physics studies.⁵⁻⁸

In the first run (Ref. 1) measurements were made on carbon for K^+ mesons from 1.0 to 2.4 GeV/c. The carbon target consisted of two pieces of equal thickness, one placed at each end of the dummy hydrogen target. In the second run (Ref. 2) measurements were made on carbon and copper

for K^+ mesons from 1.55 to 3.3 GeV/c and for \bar{p} 's from 1.6 to 3.25 GeV/c. In the second run the copper target and both parts of the carbon target were located downstream from the hydrogen target.

Table I gives the target thicknesses and the distances from the front of the transmission counters to the center of the targets. Further experimental details can be obtained from Refs. 1 and 2.

In each of the two experiments, the primary aim was the measurement of total cross sections in hydrogen and deuterium using the transmission method. Consequently, the geometry was not optimized for a transmission measurement from complex nuclei. This can be seen in Fig. 1, where the computed diffraction cross sections are shown for copper at 1.0, 2.0, and 3.0 GeV/c. The angles subtended by the transmission counters are indicated. Above about 2 GeV/c the first diffraction peak for scattering from the copper nucleus was covered by the smallest of the transmission count-

TABLE I. Target thicknesses and distances of front of transmission counters from center of targets.

Target material	Thickness (g cm ⁻²)	Distance of transmission counters from target	
		Experiment 1 (cm)	Experiment 2 (cm)
carbon	10.77	248	161.8
copper	8.18	...	161.8

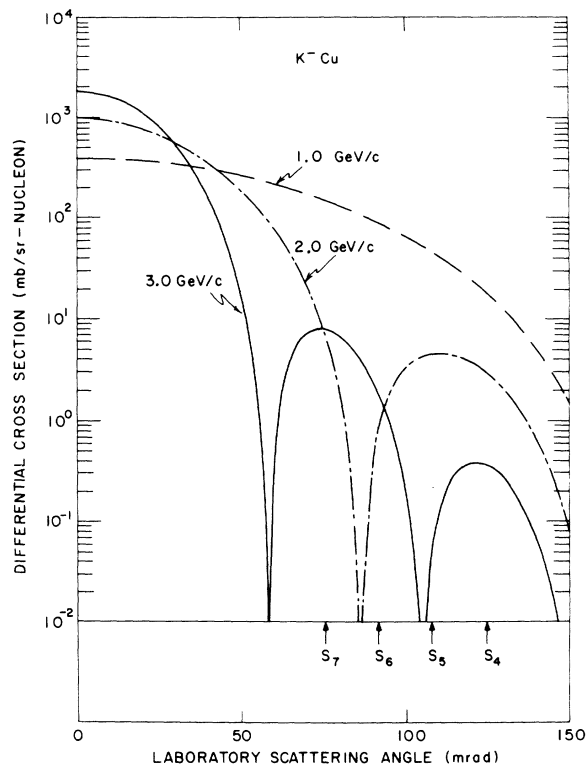


FIG. 1. Computed differential cross sections in the laboratory for diffraction scattering of K^- mesons from the copper nucleus. The values of the parameters used in the optical-model calculations were $c = 4.27$ F; $z = 0.53$ F; and $\bar{\sigma} = 42.5$ mb for 1.0 GeV/c, 27.6 mb for 2.0 GeV/c, and 24.6 mb for 3.0 GeV/c. The angles subtended by the circular transmission counters are indicated by the arrows.

ers used. In this case the transmission counters measured almost purely the absorption part of the total cross section. Below 2 GeV/c, the transmission counters began to be inside the first diffraction peak and therefore measured the absorption cross section plus a part of the diffraction. The amount of diffraction measured increased with decreasing momentum. This "intermediate geometry" situation prevailed for the carbon measurements over the entire momentum range, as illustrated in Fig. 2.

The data were analyzed in the following way. The raw "partial cross sections," i.e., the cross sections measured by each transmission counter, were first corrected for beam-size effects. The amount of diffraction scattering into each counter was then computed by an optical-model calculation (see Appendix) and subtracted from each partial cross section. The resulting absorption partial cross sections were then linearly extrapolated to zero solid angle to give the absorption cross section σ_a . In order to obtain consistency between

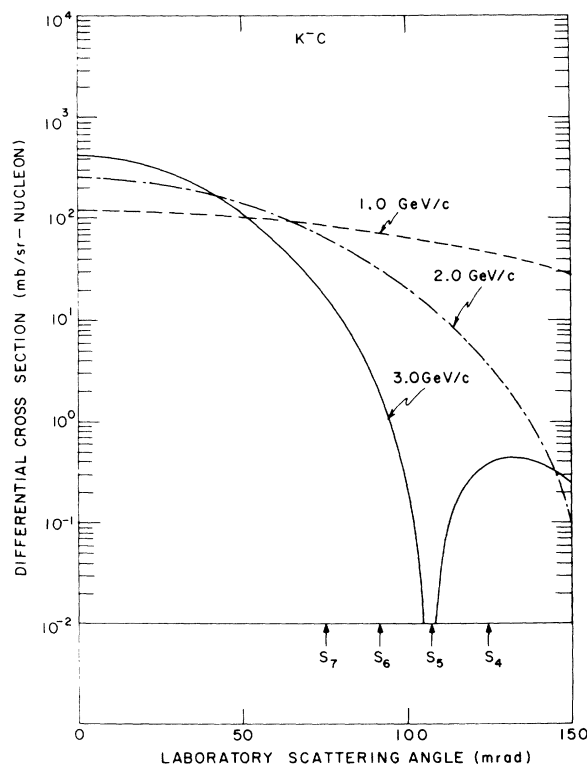


FIG. 2. Computed differential cross sections in the laboratory for diffraction scattering of K^- mesons from the carbon nucleus. The values of the parameters used in the optical-model calculations were $c = 2.29$ F; $z = 0.45$ F; and $\bar{\sigma} = 40.3$ mb for 1.0 GeV/c, 28.0 mb for 2.0 GeV/c, and 24.8 mb for 3.0 GeV/c. The angles subtended by the circular transmission counters used in the second run are indicated by the arrows.

the optical-model predictions for σ_a (see Appendix) and the experimental results, the parameter $\bar{\sigma}$, the average nucleon total cross section, was varied until σ_a computed from the optical model was in agreement with the extrapolated value.

In this analysis, it has been assumed that the missing part of the total cross section due to scattering inside the smallest transmission counter is made up of a small contribution from the absorption cross section, which extrapolates linearly to zero solid angle, and of a larger contribution from the diffraction cross section, which has been computed from the optical model. This approximation is expected to be adequate because the differential cross section at such forward angles is known to be essentially diffractive. Effects arising from Coulomb-nuclear interference scattering were neglected.

The predictions of the optical model for the differential cross sections for diffraction scattering have been given in Fig. 1 for K^- on copper and in Fig. 2 for K^- on carbon. In Fig. 3, the predic-

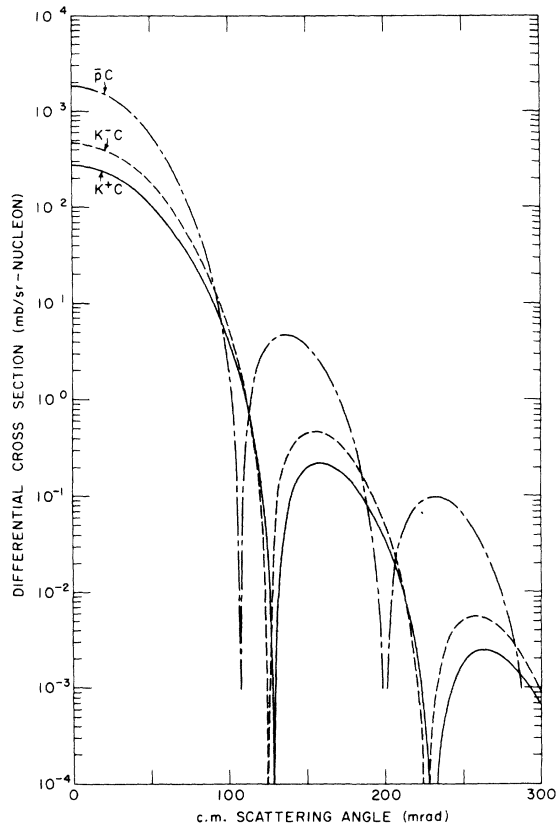


FIG. 3. Computed differential cross sections in the center-of-mass system for diffraction scattering from the carbon nucleus at 3.25 GeV/c. The values used for $\bar{\sigma}$ were 17.4 mb for K^+ mesons, 24.3 mb for K^- mesons, and 70.1 mb for \bar{p} 's.

tions are shown (in the c.m. system) for K^+ , K^- , and \bar{p} on carbon. As a check on the optical-model calculation, the computed differential elastic proton-carbon cross sections at 1.696 GeV/c are compared in Fig. 4 with the experimental results of Palevsky *et al.*⁷ The good agreement gives us confidence in the technique. A more sophisticated calculation such as those based on multiple-scattering models⁸ was not needed for the present analysis.

Tables II, III, and IV give the results for K^- -meson, K^+ -meson, and \bar{p} scattering on copper; Tables V, VI, and VII give the results for K^- -meson, K^+ -meson, and \bar{p} scattering on carbon. The results are also shown in Fig. 5. The behavior versus laboratory momentum of the various absorption cross sections is clearly related to the elementary nucleon cross sections. None of the small structures which exist in the free-nucleon cross sections is seen in the nuclear case, since they are smoothed out by the Fermi motion of the nucleons inside the nuclei and by rescattering effects. In fact, the nuclear cross sections

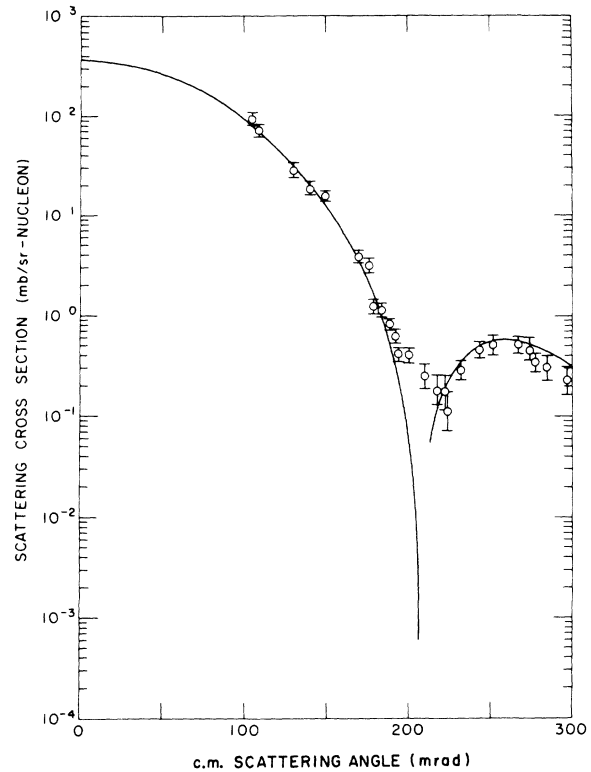


FIG. 4. Prediction of the optical model (solid curve) for proton-carbon scattering at 1.696 GeV/c, compared with the experimental results of Palevsky *et al.*⁷ The optical-model parameters used in the calculation were $c = 2.29$ F, $z = 0.45$ F, and $\bar{\sigma} = 45$ mb.

above 1.3 GeV/c are smooth and slowly decreasing functions of the laboratory momentum.

The errors listed in the tables and shown in the figures represent statistical standard deviations only. The measured partial cross sections have an estimated systematic uncertainty of about $\pm 1\%$. A larger systematic error arises in the computation of the absorption (or total) cross sections via the optical-model calculations. Since the copper measurements required very small corrections to obtain the absorption cross sections, the systematic error on σ_a due to the diffraction scattering should be relatively small. We estimate that σ_a on copper has a total systematic error of $\pm 2\%$. The computed diffraction cross section is model-dependent and may have a systematic error as large as $\pm 10\%$. Consequently, the total cross section may have a systematic uncertainty of about $\pm 4\%$.

For the carbon cross sections the optical-model corrections are larger, since the measured cross sections lie in between the absorption and total cross sections. The total systematic uncertainty for the absorption cross sections, due to instru-

TABLE II. Cross sections of K^- mesons on copper. The errors quoted represent statistical standard deviations. The systematic errors are discussed in the text.

Laboratory momentum (GeV/c)	Observed absorption cross section (mb/nucleon)	Computed diffraction cross section (mb/nucleon)	Total cross section (mb/nucleon)
1.55	12.2±0.4	6.5	18.7
1.75	11.9±0.3	6.0	17.9
2.35	11.8±0.2	5.9	17.7
2.40	11.6±0.2	5.7	17.3
2.45	11.8±0.1	5.9	17.7
2.50	11.6±0.1	5.6	17.2
2.55	11.4±0.2	5.4	16.8
2.60	11.4±0.1	5.4	16.8
2.65	11.4±0.1	5.4	16.8
2.70	11.5±0.1	5.5	17.0
2.75	11.4±0.2	5.4	16.8
2.80	11.3±0.2	5.3	16.6
2.85	11.3±0.1	5.3	16.6
2.90	11.4±0.2	5.4	16.8
2.95	11.3±0.2	5.3	16.6
3.00	11.3±0.1	5.3	16.6
3.05	11.0±0.2	5.0	16.0
3.10	10.9±0.2	4.8	15.7
3.15	11.0±0.1	4.9	15.9
3.20	10.9±0.2	4.8	15.7
3.25	10.9±0.2	4.8	15.7

TABLE III. Cross sections of K^+ mesons on copper. The errors quoted represent statistical standard deviations. The systematic errors are discussed in the text.

Laboratory momentum (GeV/c)	Observed absorption cross section (mb/nucleon)	Computed diffraction cross section (mb/nucleon)	Total cross section (mb/nucleon)
1.55	10.3±0.2	4.6	14.9
1.70	10.2±0.2	4.5	14.7
1.75	10.4±0.2	4.7	15.1
1.90	9.8±0.1	4.2	14.0
2.30	9.7±0.1	4.1	13.8
2.35	9.9±0.1	4.3	14.2
2.40	9.7±0.1	4.1	13.8
2.45	9.8±0.1	4.1	13.9
2.50	9.5±0.1	3.9	13.4
2.55	9.8±0.1	4.1	13.9
2.60	9.7±0.1	4.0	13.7
2.65	9.4±0.1	3.7	13.1
2.70	9.6±0.1	3.9	13.5
2.75	9.5±0.1	3.9	13.4
2.80	9.5±0.1	3.9	13.4
2.85	9.6±0.1	3.9	13.5
2.90	9.4±0.1	3.7	13.1
2.95	9.2±0.1	3.6	12.8
3.00	9.3±0.1	3.7	13.0
3.10	9.3±0.1	3.6	12.9
3.15	9.1±0.1	3.5	12.6
3.20	9.2±0.1	3.6	12.8
3.25	9.2±0.1	3.6	12.8
3.30	9.2±0.1	3.6	12.8

TABLE IV. Cross sections of \bar{p} 's on copper. The errors quoted represent statistical standard deviations. The systematic errors are discussed in the text.

Laboratory momentum (GeV/c)	Observed absorption cross section (mb/nucleon)	Computed diffraction cross section (mb/nucleon)	Total cross section (mb/nucleon)
1.60	17.8 ± 0.1	13.2	40.0
1.65	17.6 ± 0.1	13.0	30.6
1.70	17.4 ± 0.1	12.8	30.2
1.75	17.6 ± 0.1	12.9	30.5
1.80	17.3 ± 0.1	12.6	29.9
1.85	17.2 ± 0.1	12.5	29.7
1.90	17.1 ± 0.1	12.4	29.5
1.95	17.1 ± 0.1	12.4	29.5
2.00	17.0 ± 0.1	12.3	29.3
2.05	17.0 ± 0.1	12.2	29.2
2.10	16.9 ± 0.1	12.2	29.1
2.15	17.0 ± 0.1	12.3	29.3
2.20	17.0 ± 0.1	12.4	29.4
2.25	16.8 ± 0.1	12.1	28.9
2.30	16.7 ± 0.1	11.9	28.6
2.35	16.7 ± 0.1	12.0	28.7
2.40	16.8 ± 0.1	12.1	28.9
2.45	16.6 ± 0.1	11.8	28.4
2.50	16.5 ± 0.1	11.8	28.3
2.55	16.5 ± 0.1	11.8	28.3
2.60	16.5 ± 0.1	11.7	28.2
2.65	16.5 ± 0.1	11.7	28.2
2.70	16.6 ± 0.1	11.8	28.4
2.75	16.4 ± 0.1	11.7	28.1
2.80	16.4 ± 0.1	11.7	28.1
2.85	16.3 ± 0.1	11.6	27.9
2.90	16.2 ± 0.1	11.5	27.7
2.95	16.2 ± 0.1	11.4	27.6
3.00	16.2 ± 0.1	11.5	27.7
3.05	16.1 ± 0.1	11.3	27.4
3.10	16.1 ± 0.1	11.3	27.4
3.15	15.9 ± 0.1	11.1	27.0
3.20	15.9 ± 0.1	11.1	27.0
3.25	15.9 ± 0.1	11.1	27.0

mentals, optical-model calculations, and normalizations between the two runs, is estimated to be $\pm 2\%$ for momenta above 2 GeV/c. Below 2 GeV/c, the systematic error increases to a value of about $\pm 6\%$ at 1 GeV/c. Since the computed diffraction cross section may have an error of $\pm 10\%$, the total cross-section systematic uncertainty increases from $\pm 4\%$ at high momenta to $\pm 7\%$ at lower momenta.

A comparison of our data with those of Bugg *et al.*⁹ shows that our total cross sections are somewhat larger (about 3% for K^+ and about 8% for K^-). They have used a different method for calculating the contribution from diffraction scattering at small angles, which may account for the discrepancy.

A simple interpretation of the data may be made

in terms of the formula

$$\sigma_a = \sigma_0 A^\alpha.$$

By choosing interpolated values of the absorption cross sections at 3.2 GeV/c, one obtains the results tabulated in Table VIII. These results are consistent with those found at 10–40 GeV/c.^{10, 11} While σ_0 increases for the particles with larger elementary cross sections, α decreases. For a black nucleus one should obtain $\alpha = \frac{2}{3}$. The results of Table VIII may indicate that the nuclei are black to antiprotons but not to K^- and K^+ .

We would like to thank G. Munoz, O. Thomas, H. Sauter, and F. Seier for their technical assistance, and the members of the AGS staff for their cooperation during this experiment. We acknowl-

TABLE V. Cross sections of K^- mesons on carbon. The errors quoted represent statistical standard deviations. The systematic errors are discussed in the text.

Laboratory momentum (GeV/c)	Observed absorption cross section (mb/nucleon)	Computed diffraction cross section (mb/nucleon)	Total cross section (mb/nucleon)
0.975	22.9±1.5	9.5	32.4
1.05	22.8±0.7	9.4	32.2
1.10	23.5±0.5	10.2	33.7
1.125	22.5±0.5	9.1	31.6
1.15	22.7±0.3	9.3	32.0
1.175	21.8±0.4	8.4	30.2
1.20	21.8±0.3	8.4	30.2
1.225	21.7±0.3	8.3	30.0
1.25	20.7±0.2	7.4	28.1
1.275	20.8±0.3	7.4	28.2
1.30	20.7±0.2	7.4	28.1
1.325	20.3±0.3	7.1	27.4
1.35	20.1±0.2	6.9	27.0
1.375	20.0±0.2	6.8	26.8
1.40	19.9±0.2	6.7	26.6
1.45	19.6±0.2	6.5	26.1
1.50	19.4±0.2	6.4	25.8
1.55	19.4±0.2	6.4	25.8
1.60	19.0±0.2	6.0	25.0
1.65	19.2±0.2	6.2	25.4
1.70	18.8±0.1	5.9	24.7
1.75	19.0±0.1	6.1	25.1
1.80	18.7±0.1	5.8	24.5
1.85	18.5±0.1	5.7	24.2
1.90	18.4±0.1	5.6	24.0
1.95	18.3±0.1	5.6	23.9
2.00	18.1±0.1	5.4	23.5
2.05	18.0±0.1	5.4	23.4
2.10	18.0±0.1	5.3	23.3
2.15	18.1±0.1	5.4	23.5
2.20	18.4±0.2	5.6	24.0
2.25	17.7±0.2	5.1	22.8
2.30	18.2±0.2	5.5	23.7
2.35	17.8±0.2	5.2	23.0
2.40	17.6±0.1	5.1	22.7
2.45	17.7±0.1	5.1	22.8
2.50	17.4±0.2	4.9	22.3
2.55	17.6±0.2	5.1	22.7
2.60	17.7±0.2	5.1	22.8
2.65	17.1±0.2	4.7	21.8
2.70	17.1±0.2	4.7	21.8
2.75	16.9±0.2	4.6	21.5
2.80	17.1±0.2	4.7	21.8
2.85	16.9±0.2	4.6	21.5
2.90	16.9±0.2	4.6	21.5
2.95	16.8±0.2	4.5	21.3
3.00	16.8±0.2	4.5	21.3
3.05	17.0±0.2	4.7	21.7
3.10	16.6±0.2	4.4	21.0
3.15	16.4±0.2	4.3	20.7
3.20	16.2±0.2	4.1	20.3
3.25	16.4±0.2	4.3	20.7

TABLE VI. Cross sections of K^+ mesons on carbon. The errors quoted represent statistical standard deviations. The systematic errors are discussed in the text.

Laboratory momentum (GeV/c)	Observed absorption cross section (mb/nucleon)	Computed diffraction cross section (mb/nucleon)	Total cross section (mb/nucleon)
1.00	14.0±0.4	3.4	17.4
1.05	14.6±0.4	3.7	18.3
1.10	15.2±0.4	4.1	19.3
1.15	15.2±0.3	4.1	19.3
1.20	14.9±0.2	4.0	18.9
1.25	14.5±0.2	3.8	18.3
1.30	14.8±0.2	3.9	18.7
1.35	14.8±0.2	3.9	18.7
1.40	14.7±0.2	3.8	18.5
1.45	14.4±0.2	3.7	18.1
1.50	14.3±0.2	3.6	17.9
1.60	14.3±0.2	3.6	17.9
1.65	14.3±0.2	3.6	17.9
1.70	14.3±0.2	3.6	17.9
1.75	14.2±0.2	3.5	17.7
1.80	14.0±0.1	3.4	17.4
1.90	13.8±0.1	3.3	17.1
1.95	13.9±0.1	3.4	17.3
2.00	13.7±0.1	3.3	17.0
2.05	13.5±0.1	3.2	16.7
2.10	13.6±0.2	3.2	16.8
2.15	13.7±0.1	3.3	17.0
2.20	13.6±0.1	3.2	16.8
2.30	13.4±0.1	3.1	16.5
2.35	13.6±0.1	3.2	16.8
2.40	13.5±0.1	3.2	16.7
2.45	13.4±0.1	3.1	16.5
2.50	13.2±0.1	3.0	16.2
2.55	13.4±0.1	3.1	16.5
2.60	13.4±0.1	3.1	16.5
2.65	13.3±0.1	3.0	16.3
2.70	13.5±0.1	3.2	16.7
2.75	13.3±0.1	3.0	16.3
2.80	13.2±0.1	3.0	16.2
2.85	13.1±0.1	2.9	16.0
2.90	13.0±0.1	2.9	15.9
2.95	12.9±0.1	2.9	15.8
3.00	12.9±0.1	2.9	15.8
3.10	12.8±0.1	2.8	15.6
3.15	12.8±0.1	2.8	15.6
3.20	12.9±0.1	2.9	15.8
3.25	12.7±0.1	2.7	15.4
3.30	12.6±0.1	2.7	15.3

TABLE VII. Cross sections of \bar{p} 's on carbon. The errors quoted represent statistical standard deviations. The systematic errors are discussed in the text.

Laboratory momentum (GeV/c)	Observed absorption cross section (mb/nucleon)	Computed diffraction cross section (mb/nucleon)	Total cross section (mb/nucleon)
1.60	33.0 ± 0.1	20.2	53.2
1.65	32.8 ± 0.1	19.9	52.7
1.70	32.9 ± 0.1	20.0	52.9
1.75	32.8 ± 0.1	19.9	52.7
1.80	32.6 ± 0.1	19.6	52.2
1.85	32.5 ± 0.1	19.5	52.0
1.90	32.4 ± 0.1	19.4	51.8
1.95	32.1 ± 0.1	19.1	51.2
2.00	32.1 ± 0.1	19.0	51.1
2.05	31.9 ± 0.1	18.9	50.8
2.10	32.0 ± 0.1	18.9	50.9
2.15	31.7 ± 0.1	18.6	50.3
2.20	31.6 ± 0.1	18.5	50.1
2.25	31.6 ± 0.1	18.5	50.1
2.30	31.2 ± 0.1	18.0	49.2
2.35	31.2 ± 0.1	18.1	49.3
2.40	31.1 ± 0.1	17.9	49.0
2.45	30.9 ± 0.1	17.8	48.7
2.50	30.8 ± 0.1	17.6	48.4
2.55	30.6 ± 0.1	17.4	48.0
2.60	30.5 ± 0.1	17.3	47.8
2.65	30.3 ± 0.1	17.1	47.4
2.70	30.2 ± 0.1	16.9	47.1
2.75	30.0 ± 0.1	16.7	46.7
2.80	30.0 ± 0.1	16.7	46.7
2.85	29.7 ± 0.1	16.4	46.1
2.90	29.5 ± 0.1	16.1	45.6
2.95	29.3 ± 0.1	16.0	45.3
3.00	29.1 ± 0.1	15.8	44.9
3.05	29.1 ± 0.1	15.8	44.9
3.10	28.9 ± 0.1	15.5	44.4
3.15	28.7 ± 0.1	15.4	44.1
3.20	28.4 ± 0.1	15.1	43.5
3.25	28.3 ± 0.1	15.0	43.3

edge a number of discussions with Dr. T. Ericson, Dr. H. Goldberg, Dr. R. Rubinstein, and Dr. C. Wilkin.

APPENDIX: OPTICAL-MODEL CALCULATION

Figure 6 illustrates the variables used in the optical model. The incoming particle with an impact parameter b goes along the line AB , crossing the nucleus from C to D . The incoming particle is assumed to have small dimensions compared to those of the nucleons.

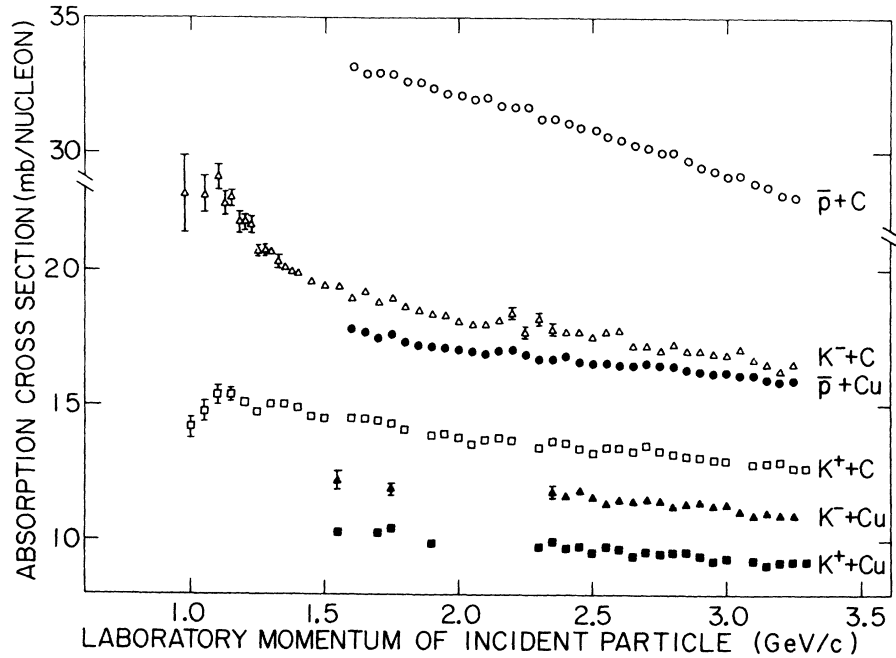
The nucleon-density distribution in nuclei was

assumed to be equal to the charge-density distribution, ρ_{em} ; in practice it is somewhat enlarged by the finite range of the nuclear forces. Electron scattering experiments¹² have shown that for medium nuclei the following Fermi distribution applies:

$$\rho_{em}(r) = \frac{\rho_0}{\exp[(r-c)/z] + 1}, \quad (1)$$

where ρ_0 is the charge density at the center of the nucleus, c is the half-density radius, and z is the falloff parameter. The electron scattering data¹² have given

FIG. 5. The absorption cross sections for K^\pm mesons and \bar{p} 's on carbon and copper.



$$c = 2.29 \text{ F}, \quad z = 0.45 \text{ F} \text{ for carbon,}$$

(2)

$$c = 4.27 \text{ F}, \quad z = 0.53 \text{ F} \text{ for copper.}$$

The normalization ρ_0 is chosen such that

$$\left(\frac{d\sigma}{d\Omega} \right)_d = \left| K_0 \int_0^\infty \{ 1 - \exp[-\bar{\sigma} \rho_0 S(b)(1 - i\bar{\alpha})] \} J_0(K_0 b \sin \theta) b \, db \right|^2, \quad (4)$$

$$\sigma_d = 2\pi \int_0^\infty \{ 1 - \exp[-\bar{\sigma} \rho_0 S(b)(1 - i\bar{\alpha})] \}^2 b \, db, \quad (5)$$

$$\sigma_a = 2\pi \int_0^\infty \{ 1 - \exp[-2\bar{\sigma} \rho_0 S(b)] \} b \, db, \quad (6)$$

where $(d\sigma/d\Omega)_d$ and σ_d are the differential and total diffraction cross sections; σ_a is the absorption cross section; b is the impact parameter (see Fig. 6); K_0 is the incoming momentum; J_0 is the Bessel

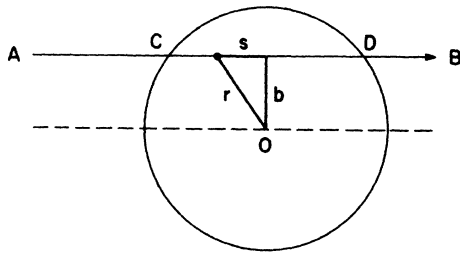


FIG. 6. Illustration of the variables used in the optical-model calculations. AB is the trajectory of the incident particle; it traverses the nucleus from C to D ; b is the impact parameter.

$$4\pi \int_0^\infty \rho(r) r^2 dr = A, \quad (3)$$

where A is the atomic weight. These density functions for carbon and copper are shown in Fig. 7.

The optical model gives the following results:

function of zeroth order; $\bar{\alpha}$ is the average value of the ratio of the real to the imaginary part of the nucleon scattering amplitude; $\bar{\sigma}$ is the average nucleon cross section. The quantity $S(b)$ is the integral

$$S(b) = \int_0^\infty \frac{1}{\exp[(r-c)/z] + 1} ds, \quad (7)$$

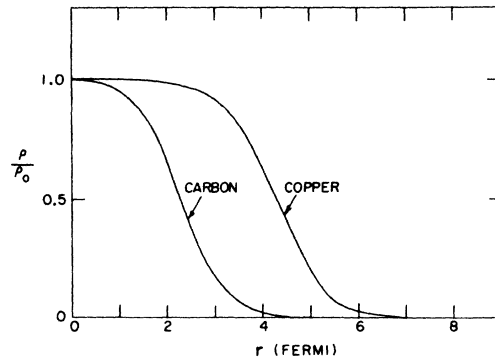


FIG. 7. The nucleon-density distributions for carbon and copper, computed from formulas (1), (2), and (3).

TABLE VIII. Average values of σ_0 and α at 3.2 GeV/c, assuming a dependence of the type $\sigma_a = \sigma_0 A^\alpha$.

Incoming particle	σ_0 (mb)	α
\bar{p}	68 ± 7	0.65 ± 0.01
K^-	29 ± 3	0.76 ± 0.01
K^+	21 ± 2	0.80 ± 0.01

where the variables s , b , and r are illustrated in Fig. 6. Figure 8 shows the results of the computation of $S(b)$ for carbon and copper nuclei.

The momentum dependence of the absorption and diffraction cross sections in Eqs. (5) and (6) is contained only in $\bar{\alpha}$ and $\bar{\sigma}$. The values used for $\bar{\alpha}$ were the same as those used in Ref. 1. A first approximation for $\bar{\sigma}$ is given by

$$\bar{\sigma} = \frac{Z\sigma_T(p) + (A-Z)\sigma_T(n)}{A}, \quad (8)$$

where Z and A are the atomic number and atomic weight of the nucleus, respectively, and $\sigma_T(p)$ and $\sigma_T(n)$ are the total cross sections of the incident particle on free protons and free neutrons, respectively. A better approximation is obtained by using, instead of the free-nucleon cross sections, the values smeared over the Fermi momentum distribution of nucleons inside the nucleus. For convenience, we have used $\sigma_T(p)$ and $\sigma_T(n)$ smeared

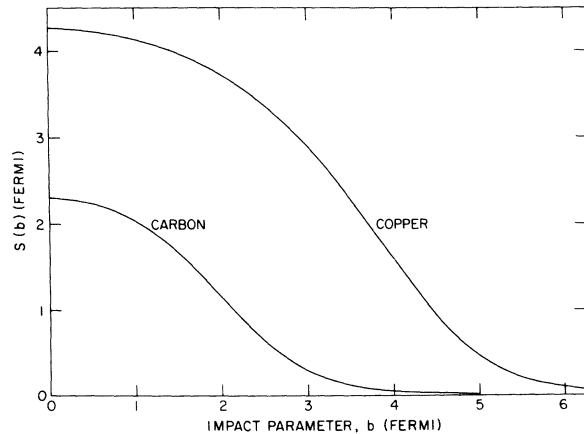


FIG. 8. The integral $S(b)$ for carbon and copper, computed from formula (7).

according to the deuteron wave function^{1,2} in (8). This was used as a starting value for $\bar{\sigma}$. In the data analysis, $\bar{\sigma}$ was varied to give consistency between the optical-model prediction for σ_a , formula (6), and the value obtained from the data. In principle, this consistency condition could allow a determination of the parameter c , the half-density radius of the nucleus for the given interaction. In view of uncertainties in deducing $\bar{\sigma}$ from the free-nucleon cross sections,⁵ it was felt that such a computation would not be appropriate with the present data.

*Work supported by the U.S. Atomic Energy Commission.

†Present address: University of Illinois at Chicago Circle, Chicago, Ill.

‡Present address: Rockefeller University, New York, N.Y.

§On leave of absence from the University of Bologna, Bologna, Italy.

|| Present address: Institut za Fiziku Sveucilista, Zagreb, Yugoslavia.

**Present address: CERN, Geneva, Switzerland.

†† Present address: CEN Saclay, Gif-sur-Yvette, France.

¹R. L. Cool, G. Giacomelli, T. F. Kycia, B. A. Leontic, K. K. Li, A. Lundby, and J. Teiger, Phys. Rev. Letters **16**, 1228 (1966); **17**, 102 (1966); R. L. Cool, G. Giacomelli, T. F. Kycia, B. A. Leontic, K. K. Li, A. Lundby, J. Teiger, and C. Wilkin, Phys. Rev. D **1**, 1887 (1970).

²R. J. Abrams, R. L. Cool, G. Giacomelli, T. F. Kycia, B. A. Leontic, K. K. Li, and D. N. Michael, Phys. Rev. Letters **18**, 1209 (1967); **19**, 249 (1967); **19**, 678 (1967); Phys. Rev. D **1**, 1917 (1970).

³C. Rubbia and J. Steinberger, Phys. Letters **23**, 167 (1966).

⁴R. W. Williams, Rev. Mod. Phys. **36**, 815 (1964).

⁵J. W. Cronin, R. Cool, and A. Abashian, Phys. Rev. **107**, 1121 (1957).

⁶T. Ericson, USAEC Report No. TID-24667, 1967 (unpublished).

⁷H. Palevsky, J. L. Friedes, R. J. Sutter, G. W. Bennett, G. J. Igo, W. D. Simpson, G. C. Phillips, D. M. Corley, N. S. Wall, R. L. Stearns, and B. Gottschalk, Phys. Rev. Letters **18**, 1200 (1967).

⁸R. J. Glauber, in *Lectures in Theoretical Physics*, edited by W. E. Brittin *et al.* (Interscience, New York, 1959), Vol. I, p. 315; *High Energy Physics and Nuclear Structure* (North-Holland, Amsterdam, 1967), p. 311; A. Y. Abul-Magd, G. Alberi, and L. Bertocchi, Phys. Letters **30B**, 182 (1969).

⁹D. V. Bugg, R. S. Gilmore, K. M. Knight, D. C. Salter, G. H. Stafford, E. J. N. Wilson, J. D. Davies, J. D. Dowell, P. M. Hattersley, R. J. Homer, A. W. O'Dell, A. A. Carter, K. F. Riley, and R. J. Tapper, Phys. Rev. **168**, 1466 (1968).

¹⁰W. Galbraith, E. W. Jenkins, T. F. Kycia, B. A. Leontic, R. H. Phillips, A. L. Read, and R. Rubinstein, Brookhaven National Laboratory Internal Report No. BNL 11598, 1967 (unpublished).

¹¹J. V. Allaby, Yu. B. Bushnin, S. P. Denisov, A. N. Diddens, R. W. Dobinson, S. V. Donskov, G. Giacomelli, Yu. P. Gorin, A. Klovning, A. I. Petrukhin, Yu. D. Prokoshkin, R. S. Shuvalov, C. A. Stahbrandt, and D. A. Stoyanova, Yadern. Fiz. **12**, 538 (1971) [Soviet J. Nucl. Phys. **12**, 295 (1971)].

¹²R. Hofstadter, Rev. Mod. Phys. **28**, 214 (1956).